Supporting Information

Identification of Novel GPR55 Modulators Using Cell-Impedance-Based Label-Free Technology

Paula Morales,[#] Lauren Whyte,[¶] Roberto Chicharro,[#,†] María Gómez-Cañas,[§,$,£] M. Ruth Pazos, [§,$,£] Pilar Goya,[#] Andrew J. Irving,[₸] Javier Fernández-Ruiz, [§,$,£] Ruth A. Ross,[¶,*] and Nadine Jagerovic[#,*]

TABLE OF CONTENTS

Conformational analysis and electrostatic potential map calculation.

Previous to the synthesis of our two proposed series of compounds (series I and series II), conformational analysis of two pyrazole isomers from each series was performed using ab initio Hartree-Fock (HF) calculations at the 6-31G* level within the Spartan '08 (Wave function, Inc., Irvine, CA). A conformational search was next implemented using Molecular Mechanics (Monte Carlo method). Local energy minima was identified by rotation of a subject torsion angle through 360 in 60 increments (6-fold search), followed by HF 6-31G* energy minimization of each rotamer generated. The electrostatic potential of the global minimum energy conformer was calculated using the Hatree-Fock method at the 6-31G* level of theory and was mapped on the 0.002 isodensity surface of each molecule. The surface was color-coded according to the potential, with electron rich regions colored red and electron poor regions colored blue.

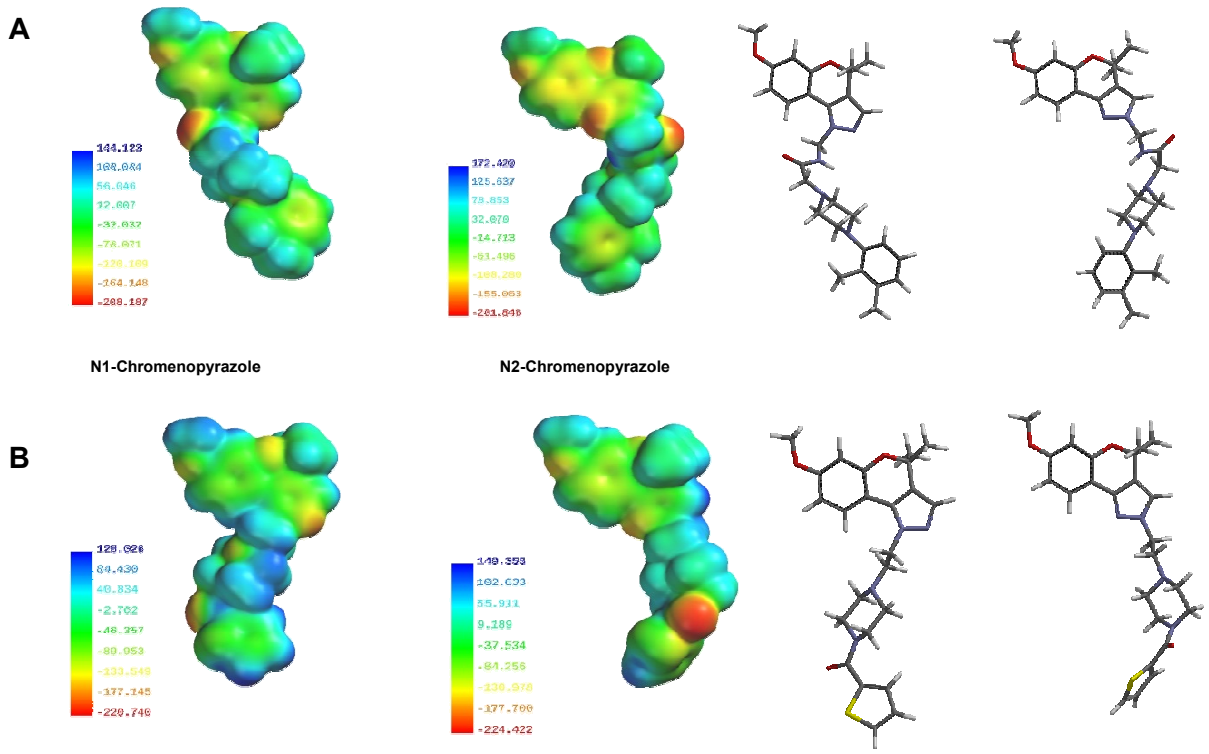

Figure S1: A) N1- and N2-(4-(2,3-dimethylphenyl)piperazinyl)acetamidomethyl chromenopyrazole (Series I) electrostatic potential maps and minimized conformers used to calculate the map. B) N1- and N2-(4-(2-thenoyl)piperazinyl)ethylchromenopyrazole (Series II) electrostatic potential maps and minimized conformers used to calculate the map. The electrostatic potential scale (in kJ/mol) is provided as a color scale. This scale is from blue (most electropositive) to red (most electronegative).

In a first approximation, this study suggests the inverted-L shape adopted by compounds from both series with a high electronegative region nearby the chromenopyrazole head region for series I corresponding to the amide carbonyl group, and a high electronegative region located in the end of the central area for series II corresponding to the acyl carbonyl group. These structural features agree with Reggio's data. They suggested GPR55 agonism for compounds of series I

and GPR55 antagonism for series II. Therefore, chromenopyrazole as scaffold was expected to be attractive.

***In silico* ADME properties.**

Table S1. Physicochemical descriptors calculated by QikProp 3.5 integrated in Maestro (Schrödinger, LLC, New York, USA) [range of 95% of drugs].

Compd	QPlogS[a]	QlogBB[b]	QPlogHERG[c]	QPPCaco[d]	%Human oral absorption GI[e]
13a	-4.8	0.11	-5.803	529	100
13b	-4.7	0.10	-6.064	504	100
14a	-4.8	0.05	-5.588	529	100
14b	-4.7	0.04	-5.842	504	100
15a	-5.5	0.10	-5.543	529	100
15b	-5.5	0.09	-5.789	504	100
16	-4.5	0.06	-5.395	529	100
18a	-4.1	-0.05	-6.779	559	100
18b	-4.1	0.08	-7.051	774	100
19a	-4.7	0.01	-7.076	641	100
19b	-5.2	0.08	-7.524	796	100
20a	-4.8	0.12	-6.755	642	100
20b	-4.9	0.25	-7.085	880	100
21	-4.4	0.03	-6.334	589	100
22	-2.9	0.13	-5.028	512	89
23	-4.6	0.30	-5.133	832	100
24	-3.9	0.27	-5.041	750	100
LPI	-3.4	-4.84	-4.139	5	11

[a]Predicted aqueous solubility [-6.5/0.5]; bPredicted log of the brain/blood partition coefficient [-3.0/1.2]; cHERG K+ Channel Blockage (log IC50) [concern below -5]; dApparent Caco-2 cell permeability in nm/s [<25 poor, >500 excellent]; eHuman Oral Absorption in GI [<25% is poor].

Impedance-based cellular assays: Concentration-respo–nse curves of 19b, 20b, 22, 23, and 24 compared to LPI; Concentration-response curves of LPI in presence of 2224 in hGPR55-HEK293 cells using xCELLigence system.

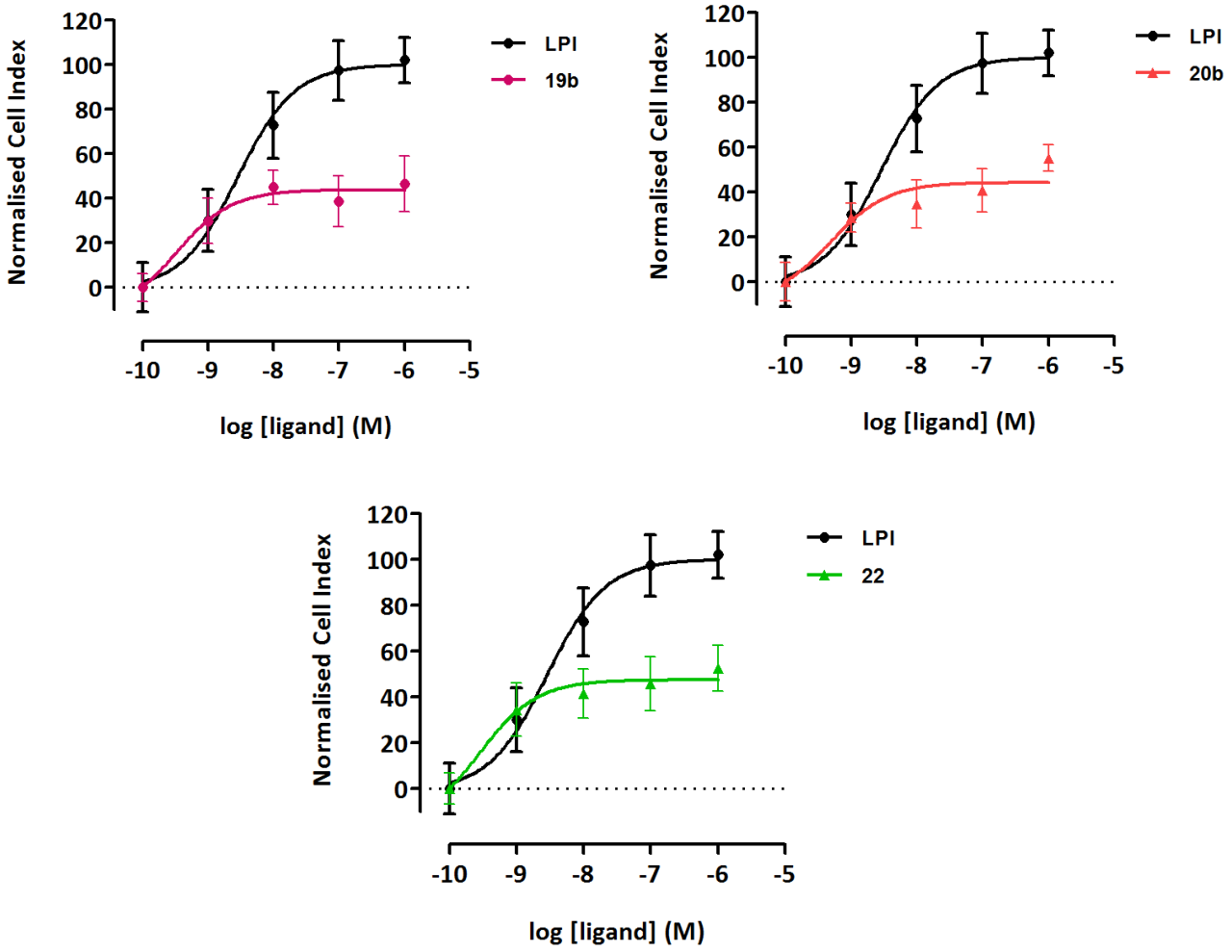

Figure S2. A. Concentration-response curves of **19b** (upper right), **20b** (upper left), and **22** (lower) in hGPR55-HEK293 cells using xCELLigence system. Data points represent the mean ± SEM values of four independent experiments, performed in duplicate. The data is presented as a percentage of the maximal LPI stimulation (at 1 μM, LPI displays off-target activity at 10 μM).

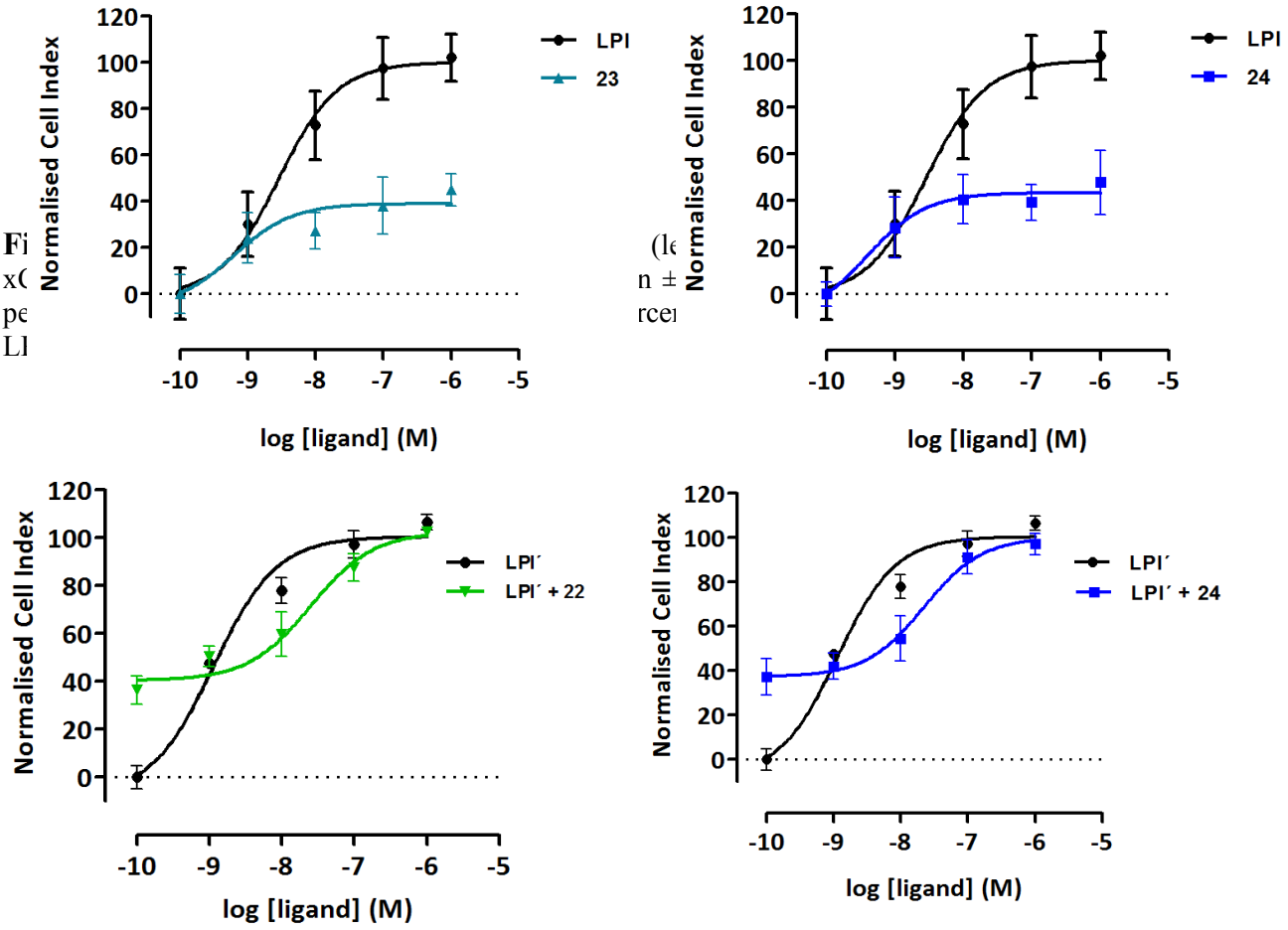

Figure S4. Concentration-response curves of LPI in the presence and absence of **22** (left) and **24** (right) in hGPR55-HEK293 cells using xCELLigence system. Data points represent the mean ± SEM values of at least four independent experiments, performed in duplicate. The data is presented as a percentage of the maximal LPI stimulation.

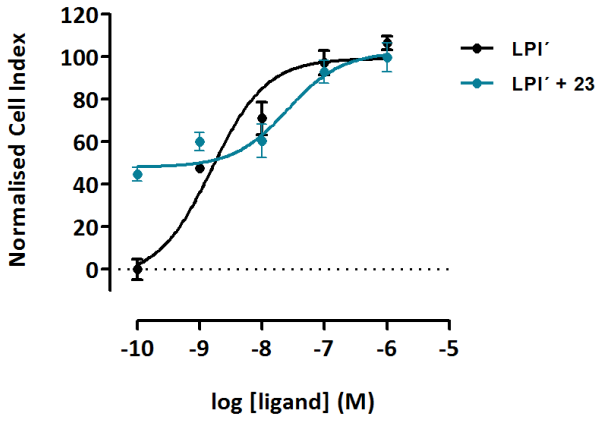

Figure S5. Concentration-response curves of LPI in the presence and absence of **23** in hGPR55-HEK293 cells using xCELLigence system. Data points represent the mean ± SEM values of at least four independent experiments, performed in duplicate. The data is presented as a percentage of the maximal LPI stimulation.

Chemistry: Supporting Information

7-Methoxy-2,2-dimethylchroman-4-one (2).[1] To a solution of 2-hydroxy-4-methoxyacetophenone (3.01 g, 18.0 mmol) in ethanol (30 mL) and acetone (13.2 mL, 180.5 mmol), pyrrolidine (4.5 mL, 54.2 mmol) was added in one portion. The mixture was refluxed for 6 h. After reaction completion, the solvent was removed under reduced pressure. The resultant crude was diluted by EtOAc and washed with aqueous NH_4Cl solution and brine. The aqueous layer was extracted with EtOAc three times. The combined organic layer was dried over anhydrous $MgSO_4$, filtered and the solvent was condensed under vacuum. Column chromatography on silica gel (hexane/ EtOAc, 3:1) provided the desired product as a yellow solid (3.04 g, 82%); mp: 81–83ºC (82-83ºC);[2] ^{1}H-NMR (400 MHz, $CDCl_3$) δ: 7.78 (d, J = 8.8 Hz, 1H, 5-H), 6.52 (dd, J = 8.8, 2.4 Hz, 1H, 6-H), 6.36 (d, J = 2.4 Hz, 1H, 8-H), 3.81(s, 3H, OCH3), 2.66 (s, 2H, 3-H), 1.44 ppm (s, 6H, $OC(CH_3)_2$); 13C-NMR (101 MHz, $CDCl_3$) δ: 191.3 (4-C), 166.4 (7-C), 162.2 (8a-C), 128.4 (5-C), 114.3 (4a-C), 109.5 (8-C), 101.3 (6-C), 79.8 (2-C), 55.8 (OCH_3), 48.8 (3-C), 26.9 ppm ($OC(CH_3)_2$); HPLC-MS: [A, 15→95%], t_R: 4.55 min, (100%); MS (ES^+, m/z) 207 $[M + H]^+$.

3-(Hydroxymethylene)-7-methoxy-2,2-dimethylchroman-4-one (3).[3] A solution of **2** (2.80 g, 13.6 mmol) in anhydrous THF (15 mL) was added to a vial containing dry sodium hydride (1.30 g, 54.4 mmol) under N_2 atmosphere. The mixture was irradiated under microwave at 45ºC for 25 min. Subsequently, ethyl formate (5.48 mL, 68.0 mmol) was added to the sealed vial and it was irradiated under microwave at 45ºC for 25 minutes. Water was added and the product was extracted with EtOAc. The combined organic layers were dried over Mg_2SO_4 and the solvent was evaporated under reduced pressure. The crude was purified by column chromatography on silica gel (hexane/ EtOAc, 3:1) to afford the title product **3** (1.46 g, 52%) as a light yellow oil: ^{1}H-NMR (400 MHz, $CDCl_3$) δ: 7.82 (d, J = 8.7 Hz, 1H, 5-H), 7.78 (d, J = 9.0 Hz, 1H, C*H*OH),

6.49 (dd, J= 8.7, 2.1 Hz, 1H, 6-H), 6.26 (d, J = 2.1 Hz, 1H, 8-H), 3.37 (s, 3H, OCH_3), 1.45 ppm (s, 6H $OC(CH_3)_2$); ^{13}C-NMR (101 MHz, $CDCl_3$) δ: 189.6 (4-C), 167.4 (7-C), 164.2 (CHOH), 158.9 (8a-C), 126.8 (5-C), 115.1(4a-C), 110.3 (8-C), 105.8 (6-C), 87.1 (2-C), 64.5 (OCH_3), 50.9 (3-C), 25.8 ppm ($OC(CH_3)_2$); HPLC-MS: [A, 60→95%], t_R: 2.70 min, (98%); MS (ES+, *m/z*) 235 $[M + H]^+$.

1,4-Dihydro-7-methoxy-4,4-dimethylchromeno[4,3-*c*]pyrazole (4).[4] A solution of **3** (1.46 g, 6.3 mmol) and anhydrous hydrazine (0.58 mL, 18.8 mmol) in EtOH (20 mL) was stirred at 60ºC during 2 h. The solvent was removed under reduced pressure, and the crude residue was subjected to silica gel column chromatography (hexane/EtOAc, 1:1) to obtain **4** as a white solid (0.99 g, 69%); mp: 158-160ºC (167-169ºC);[4] ^{1}H-NMR (400 MHz, $CDCl_3$) δ: 7.98-7.96 (br s, 1H, NH), 7.57 (d, *J* = 7.8, Hz, 1H, 9-H), 7.33 (s, 1H, 3-H), 6.55 (d, *J* = 2.5 Hz, 1H, 6-H), 6.52 (dd, *J* = 7.8, 2.5 Hz, 1H, 8-H), 3.78 (s, 3H, OCH_3), 1.61 ppm (s, 6H, $OC(CH_3)_2$); ^{13}C-NMR (101 MHz, $CDCl_3$) δ: 161.3 (7-C), 154.6 (5a-C), 125.6 (9b-C), 123.7 (3-C), 123.1 (3a-C), 120.2 (9-C), 109.9 (8-C), 108.1 (6-C), 103.2 (9a-C), 76.2 ($OC(CH_3)_2$), 55.5 (OCH_3), 29.4 ($OC(CH_3)_2$); HPLC-MS: [A, 15→95%], t_R: 4.09 min, (98%); MS (ES+, *m/z*) 231 $[M + H]^+$.

(1) Zhu, M.; Kim, M. H.; Lee, S.; Bae, S. J.; Kim, S. H.; Park, S. B. Discovery of novel benzopyranyl tetracycles that act as inhibitors of osteoclastogenesis induced by receptor activator of NF-κB ligand. *J. Med. Chem.* **2010**, *53*, 8760–8764.

(2) Camps, F.; Coll, J.; Messeguer, A.; Pericás, M. A.; Ricart, S.; Bowers, W. S.; Soderlund, D. M. An Improved Procedure for the Preparation of 2,2-Dimethyl-4-chromanones. *Synthesis (Stuttg).* **1980**, *1980*, 725–727.

(3) An, H.; Eum, S.-J.; Koh, M.; Lee, S. K.; Park, S. B. Diversity-oriented synthesis of privileged benzopyranyl heterocycles from s-cis-enones. *J. Org. Chem.* **2008**, *73*, 1752–1761.

(4) Brown, R. E.; Shavel, J. J. Substituted Benzopyranopyrazoles **1971**, Patent US19690826656.